Protodeboronation of heteroaromatic, vinyl and cyclopropyl boronic acids: pH-rate profiles, auto-catalysis and disproportionation

Protodeboronation of heteroaromatic, vinyl and cyclopropyl boronic acids: pH-rate profiles, auto-catalysis and disproportionation

Paul A. Cox,[†] Andrew G. Leach,[‡] Andrew D. Campbell,[§] and Guy C. Lloyd-Jones*[,†]

[†] School of Chemistry, University of Edinburgh, Joseph Black Building, David Brewster Road, Edinburgh, EH9 3FJ, UK

[§] AstraZeneca, Pharmaceutical Technology and Development, Silk Road Business Park, Macclesfield, SK10 2NA, UK

[‡] School of Pharmacy and Biomolecular Sciences, Liverpool John Moores University, Byrom Street, Liverpool L3 3AF, UK

ABSTRACT: pH-rate profiles for aqueous-organic protodeboronation of 18 boronic acids, many widely viewed as unstable, have been studied by NMR and DFT. Rates were pH dependent, and varied substantially between the boronic acids, with rate maxima that varied over 6 orders of magnitude. A mechanistic model containing five general pathways (k_1-k_5) has been developed, and together with input of $[B]_{total}$, K_W, K_a and K_{aH}, the protodeboronation kinetics can be correlated as a function of pH (1-13) for all 18 species. Cyclopropyl and vinyl boronic acids undergo very slow protodeboronation, as do 3- and 4-pyridyl boronic acids ($t_{0.5}$ > 1 week, pH 12, 70 °C). In contrast, 2-pyridyl and 5-thiazolyl boronic acids undergo rapid protodeboronation ($t_{0.5}$ ≈ 25-50 sec, pH 7, 70 °C), via fragmentation of zwitterionic intermediates. Lewis acid additives (e.g. Cu, Zn salts) can attenuate (2-pyridyl) or accelerate (5-thiazolyl, and 5-pyrazolyl) fragmentation. Two additional processes compete when the boronic acid *and* the boronate are present in sufficient proportions (pH = pK_a ± 1.6): i) self-/auto-catalysis and ii) sequential disproportionations of boronic acid to borinic acid and borane.

Introduction

Boronic acids are key reagents in synthesis,[1] and ubiquitous in classic processes such as, *inter alia*, Suzuki-Miyaura,[2] oxidative Heck,[3] Chan-Evans-Lam,[4] and Liebeskind-Srogl couplings,[5] and addition to enones,[6] carbonyls and imines.[7] Boronic acid decomposition, notably by *in situ* protodeboronation,[1] compromises reaction efficiency, and motifs such as 2-heteroaryl,[8] vinyl[9] and cyclopropyl,[10] are sometimes troublesome. As a consequence, a range of techniques have been developed to mitigate decomposition during coupling,[1,11] these include highly tuned catalysts,[12] the use additives (e.g. Cu, Zn and Ag salts) sometimes proposed to act by transmetallation,[13] masked reagents,[14,] and slow release of the boronic acid *in situ*[11] from MIDA boronates[15] and trifluoroborates.[16]

Given the importance of boronic acids in Suzuki-Miyaura coupling, a process that is frequently conducted in aqueous-organic solvent media,[16c] general mechanistic understanding of direct aqueous protodeboronation is surprisingly limited. Moreover, nearly all studies have focussed on substituted phenylboronic acids.[1,12,17] The most detailed investigation was reported by Kuivila, who measured the protodeboronation kinetics of a series of $ArB(OH)_2$ species (Ar = *o*,*m*,*p*-X-C_6H_4; X = MeO, Me, Cl, and F) in aqueous buffers at 90 °C, with initial $ArB(OH)_2$ concentrations in the range 3-5 mM.[17c-f] By analysis of pH-rate profiles (between pH 1.0 and 6.7), two pathways were identified, Scheme 1. The first was a specific acid-catalysed process (k_1), shown to proceed via aromatic electrophilic substitution of B by H. The second pathway was found to be base-catalysed, and proposed to proceed via hydrolysis (k_2) of the boronate anion ($[ArB(OH)_3]^-$). This latter species is generated in a pH-determined equilibrium involving association of water (K_a)[18] or hydroxide (K_a/K_W) with the boronic acid. A key issue is that the kinetics were measured by UV-Vis spectroscopy and could not be determined above pH 6.7 due to the onset of UV-dominating boronic acid oxidation processes.[17f] As a consequence of the pH being substantially below that required to effect significant conversion of the boronic acid to the boronate, the rate constant (k_2) was calculated from k_{obs}, using an estimated value for K_a. In addition to elucidation of the two major pathways (k_1 and k_2) for aqueous protodeboronation, Kuivila's studies also identified that electron withdrawing groups, at *para* or *meta* positions on the aromatic ring, attenuate protodeboronation rates, *via* both pathways. However, whilst these studies were extensive,[17c-f] they were conducted long before the ascendency of the Suzuki-Miyaura reaction.[2] In other words, the importance of detailed study of the base-catalysed process, across the full alkaline pH range (i.e. well above pH 6.7), was not yet apparent.

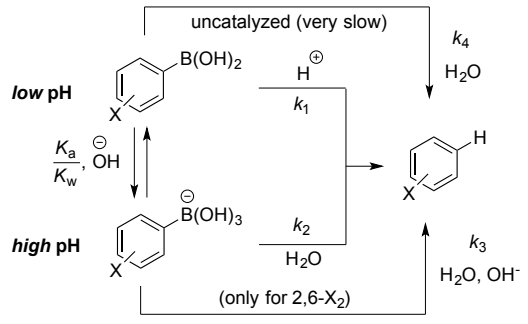

Scheme 1. Kuivila mechanisms (k_1, k_2) for $ArB(OH)_2$ protodeboronation in aqueous acidic (k_1),[17c] and basic (k_2)[17f] media. Also shown is a third pathway, involving boronate $[ArB(OH)_3]^-$ deprotonation and C-B protolysis (k_3), proposed by Perrin[17k] for substrates with 2,6-disubstitution (X = F, Cl, Br, CF_3); and an uncatalyzed pathway (k_4) involving direct reaction with (autoionized) water.

Indeed, it was only rather recently that the kinetics of protodeboronation of arylboronic acids have been studied under basic conditions. In 2002, Frohn measured protodeboronation rates of various polyfluorophenyl boronic acids in aqueous pyridine, and in aqueous basic methanol, concluding that the mechanism involved protolysis of either the boronate (i.e. k_2) or the conjugate base of the boronic acid.[17i] In 2003 Cammidge reported in detail on the effect of various anhydrous and aqueous-organic media in the protodeboronation of 2,3-difluoro-4-heptyl-6-tolyl boronic acid mediated by CsF,[17j] concluding that aqueous protolysis of the corresponding boronate was involved. In 2010 Buchwald used calorimetry to measure protodeboronation kinetics of a series of substituted 2,6-difluorophenyl boronic acids (3-F, 3-OBu, 4-F and 4-H) in a biphasic basic-aqueous medium (aq. K_3PO_4 / THF).[12] Perrin extended this study, including other electronegative 2,6-disubstituents: Cl, Br, and CF_3,[17k] which led to the proposal of a new, i.e. non-Kuivila type, mechanism involving specific-base mediated protolysis (k_3) of the boronate anion ([$ArB(OH)_3$]). The process was only found to occur with boronic acids bearing a substituent at both *ortho*-positions (i.e. 2,6-disubstitution).[17k]

Despite the core role of heteroaromatic boronic acids in synthesis and discovery, and the propensity for many to undergo protodeboronation, during storage[17i] and in coupling,[8,12] there is a near-complete absence of the kinetic data requisite for their behaviour to be compared and contrasted. Thus, whilst it is known empirically, or anecdotally, that certain heteroaromatic boronic acids are much more prone to protodeboronation than others,[1,8,11b] it is not clear whether overall they behave similarly to substituted phenylboronic acids, i.e. displaying the simple acid- and base-catalysed pH relationships (k_1, k_2) identified by Kuivila, or whether there are more complex pH dependencies for some classes of heteroaromatic boronic acids, for example involving heterocycle basicity, or other pathways, such as the specific-base mediated protolysis (k_3) identified by Perrin.[17k] Indeed, it is not even clear for an individual class of heteroaromatic boronic acid, whether extremes of pH (low or high) are to be avoided, or are beneficial, in terms of stability.

For all of the above reasons, we set out to study the intrinsic aqueous protodeboronation of a range of heteroaromatic (**2-17**), vinyl (**18**), and cyclopropyl (**19**) boronic acids, in a homogeneous organic-aqueous medium. Herein, we report the overall kinetics of their protodeboronation, but more importantly also show how the resulting pH-rate profiles can be simulated and analysed using a general kinetic model. The model extends beyond the basic Kuivila processes (k_1, k_2), by including the Perrin mechanism (k_3), plus three additional protolysis processes (k_2cat, k_4, and k_5, *vide infra*), and the requisite pH-dependent speciation equilibria for boronic acid association with water (K_a) and, if required, the protonation state of basic heterocycles (K_{aH}). The model can be used in two ways: i) as a general exploratory tool, with manual input of the requisite pH, concentrations, rates and equilibrium constants or, ii) as a means to fit experimental data, through automated numerical iteration of rate and equilibrium constants (including K_a and K_{aH}) - provided that the rate data has been acquired over a suitably wide pH range. *To assist in application of the model, a pre-configured spreadsheet is provided as part of the Supporting Information.*

The model provides the basis for quantification of the dominant protodeboronation processes occurring for different boronic acid species, at different pH and substrate concentrations. Thus, the impact of pH on the kinetics allows identification of new mechanistic regimes, and these mechanisms can then be explored in more detail using kinetics, isotopic labelling, effects of additives, and computation. Overall the study has facilitated: i) classification of the reactivity imparted by 16 different heterocyclic structures (**2-17**) between pH 1 and 13; ii) elucidation and investigation of new protodeboronation mechanisms and a competing disproportionation process; iii) preliminary details on origins of the (de)stabilizing effect of additives such as Zn and Cu salts on some heterocyclic boronic acids; and iv) identification of substrate-specific pH-stability zones, in which even notoriously unstable boronic acids, e.g. 2-pyridyl, can be stable for a few hours at 70 °C. This information will aid a more informed choice of conditions for the preparation, storage[17i] and application of boronic acids in synthesis,[1] as well as means to induce their deliberate[19] protodeboronation.

Results and discussion

1. Protodeboronation via Kuivila Mechanisms (k_1 and k_2). In preliminary studies we confirmed that the protodeboronation of a simple *para*-substituted phenyl boronic acid could be satisfactorily analysed *in situ* by $^1H/^{11}B$ NMR under aqueous conditions. Choosing *p*-anisyl boronic acid (**1**),[17c,f] protodeboronation kinetics were determined in water at 90 °C, without a malonate buffer.[17c,f] The aqueous association constant (pK_a **1** = 9.10; 90 °C) was determined by ^{11}B NMR pH-titration. Control experiments confirmed that basic solutions of **1** became pale brown in colour, with large increases observed in UV-Vis absorption spectra, as reported by Kuivila.[17f] However, the NMR spectra of such samples were unaffected: there was no sign of mequinol (*p*-hydroxy anisole) - the anticipated product of oxidation of **1**, or indeed anything other than the time-average signal from [**1**/**1**$_{OH}$] and the protodeboronation products: anisole and boric acid. The trace quantities of oxidative side product(s) are thus intensely UV-active, and possibly polymeric.

Table 1. Protodeboronation 1 and 2 at 90 °C.

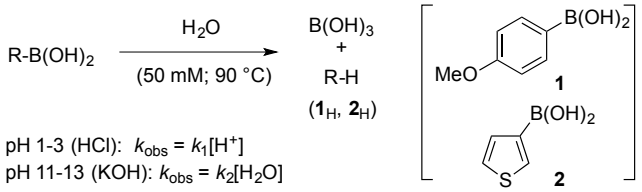

Entry	$ArB(OH)_2$	pK_a[a]	k_1 M^{-1} s^{-1}	k_2 M^{-1} s^{-1}
1	**1**	9.10	0.68×10^{-4} [b]	3.9×10^{-8} [b]
2[c]	**1**	9.60[d]	1.1×10^{-4} [e]	8.4×10^{-6} [f]
3	**2**	8.91	3.3×10^{-6} [b]	1.4×10^{-8} [b]

a) ^{11}B NMR pH titration; b) ^{11}B NMR at pH 1-3 and 11-13; c) from refs. 17c,f; d) estimated in ref. 17f. e) extrapolated from data in ref. 17c; f) from k_{obs} at pH 6.7 (25°C, uncorrected) and estimated K_a.

Using HCl and KOH to explore the acid (pH 1-3) and base (pH 11-13) regimes, protodeboronation kinetics were analysed by non-linear regression of the exponential decays observed for [**1**/**1**$_{OH}$]. The second-order rate constants (k_1 and k_2) are given in Table 1, entry 1. Kuivila's value for the limiting rate constant at

high pH (k_2, entry 2), was obtained by pH-rate extrapolation and is two orders of magnitude too large.[17k] This arises from the conflation of an overestimated pK_a for **1** (9.60), with a uncorrected pH (25 °C)[20] for the k_{obs} determination at 90 °C, and reinforces the value of full pH range rate profiling.

Moving to the protodeboronation of heterocycles, 3-thienylboronic acid (**2**) was chosen for initial studies, on the basis of its solubility, relative stability, and low basicity. Second-order rate constants (k_1 and k_2; Table 1, entry 3) were determined under the same conditions (50 mM, H_2O, 90 °C) as for *p*-anisyl boronic acid **1**. Within the limits of the pH range explored (pH 1-13), there was no detectable contribution by the base-catalysed boronate mechanism (k_3), or direct reaction of the boronic acid with H_2O (k_4; Scheme 1);[21] although both mechanisms (k_3 and k_4) were found to be important with some heterocycles, *vide infra*.

3-Thienyl boronic acid **2** is less susceptible to aromatic electrophilic substitution (k_1)[22] than **1**, but the boronates ($\mathbf{1}_{OH}$ and $\mathbf{2}_{OH}$) are of similar reactivity (k_2, Table 1 entries 1 and 3). Computational studies on this process identified rate-limiting C-protonolysis of the boronate ($\mathbf{2}_{OH}$, Figure 1, upper structure) by water. As found for all of the boronates studied, the three hydroxyl groups in $\mathbf{2}_{OH}$ preferentially adopt a distinctive triskelion conformation. Hydrogen bonding of the boronate by incoming water results in the C-B bond stretching such that, in the transition state (TS), the 3-thienyl carbanion is midpoint in its translation from the Lewis acid ($B(OH)_3$) to the Brønsted acid (OH).

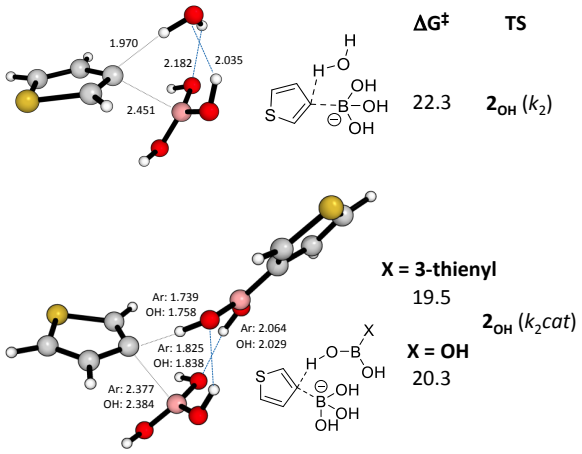

Figure 1. DFT (M06L/6-311++G**)[23-27] transition state structures for protonolysis of 3-thienylboronate $\mathbf{2}_{OH}$ by water (k_2, top) and by boronic acid (**1**, $k_2$cat, bottom) to generate $\mathbf{2}_H$ and $[B(OH)_4]^-$.

2. Auto-catalyzed Protodeboronation (k_2cat). If protodeboronation of **2** arises solely by the Kuivila mechanisms (k_1, k'_2), ($k'_2 = k_2[H_2O]$) the empirical rate equation predicts a simple pH – log k_{obs} rate profile, Figure 2. Specifically, for k'_2 (see solid line, Figure 2) the rate should rise and then reach a plateau as the pH extends above the pK_a of the boronic acid **2** (pK_a = 8.91 at 90 °C). The data deviates from this theoretical curve, the deviation being greatest at pH 8.9. This deviation was found for many of the boronic acids studied, *vide infra*, and indicates that there is an additional protodeboronation process that augments k'_2, but with a distinctly different pH-profile. A pronounced concentration dependence was noted, with the deviation from k'_2 becoming greater as the boronic acid concentration is raised (compare 0.05 M to 0.40 M, Figure 2). As the maximum deviation occurs when pH = pK_a (8.91), where the proportions of $[RB(OH)_3]^-$ and $RB(OH)_2$ are identical, analogous to that of a bimolecular Job-plot,[28] this suggest self-catalysis (k_2cat). To account for the approximately pseudo first-order kinetics (*vide infra*), the product ($B(OH)_3$) needs to be similarly effective an auto-catalyst,[29] as the boronic acid is a self-catalyst.[17l] This was confirmed by addition of 350 mM $^{10}B(OH)_3$ to the protodeboronation of 50 mM **2**. At pH 8.90, ^{11}B-NMR analysis afforded the same pseudo first-order rate constant as for 400 mM **2** alone ($[B]_{tot}$ = 400 mM in both cases). Using an augmented rate equation containing k_2cat allows satisfactory kinetic simulations (dashed lines in Figure 2). DFT transition state energies, confirmed that water can be replaced by boronic acid **2** (Figure 1, lower structure) or boric acid as proton sources, and KIEs determined from reactions in D_2O (Figure 2, inset) confirm rate-limiting proton-transfer.

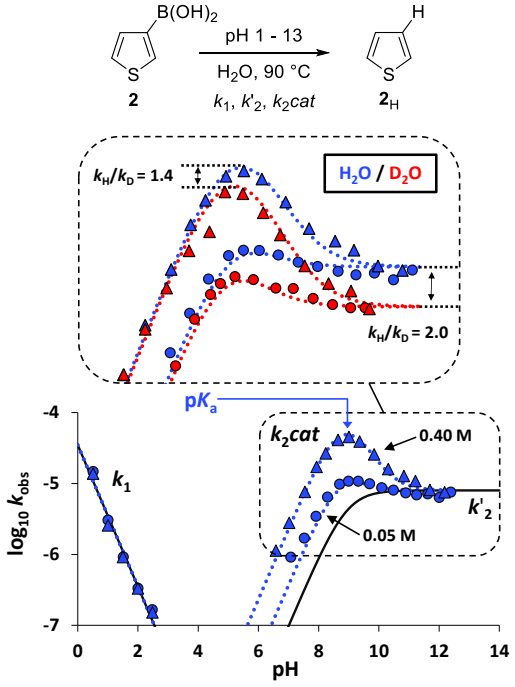

Figure 2. Effect of pH and concentration on the rate of protodeboronation of thienyl boronic acid **2**. Dashed lines: k_{obs} = $((k'_2 + k_2cat[B]_{tot})/(1+10^{(pKa-pH)}))$ + $((k_1/10^{pH})/(1+10^{(pH-pKa)}))$ values as Table 1, entry 3, plus k_2cat = 6.2 ×10^{-5} $M^{-1}s^{-1}$; for solid line, k_2cat = 0. Inset shows rate profile in D_2O (red), using an x-axis scale of pD + ΔpK_W to account for the change in water auto-ionization (K_W).[30] pK_a **2** (^{11}B NMR pH titration, 90 °C): 8.91 (H_2O) and 9.68 (D_2O).

3. B-OH-catalyzed Disproportionation. After some preliminary investigation with heterocyclic boronic acids, a mixture of H_2O/1,4-dioxane (1:1) at 70 °C was found to provide the best combination of substrate solubility (50 mM) while remaining fully homogeneous at the wide range of base, salt, buffer, additive and acid concentrations required to usefully explore the pH range (1-13). With higher initial concentrations of boronic acid, some substrates displayed small deviations from pseudo-first-order protodeboronation kinetics when carefully monitored at pH = pK_a ± 0.1.

This deviation had already been observed with thienyl boronic acid **2** in H_2O at 90 °C, *vide supra*, and together with tests for boryl exchange at the aryl ring, Scheme 2, indicated that processes in addition to k_2cat occur when *both* $[RB(OH)_3]^-$ and $RB(OH)_2$ are present at high concentration (pH = pK_a).

Scheme 2. ^{10}B / ^{11}B exchange. Reaction of $^{11}B(OD)_3$ (0.2 M) with [^{10}B]-**2**$_{OD}$ (0.2 M) to generate small quantities of [^{11}B]-**2**/[^{11}B]-**2**$_{OD}$ and $^{10}B(OD)_3$ ($^{10/11}$B-NMR, D_2O, 90 °C). Regioisomer **3** protodeboronates without significant disproportionation.

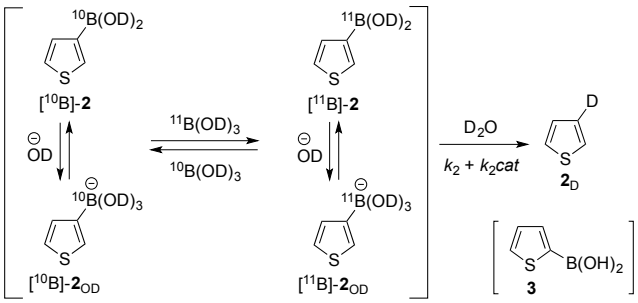

^{11}B-NMR analyses of this process indicated other transient minor (≤ 5 %) species to be present, and the pH shift dependency of one of these species suggested it to be a borinate,[31] [(3-thienyl)$_2$B(OH)$_2$]$^-$, generated by disproportionation of **2**/**2**$_{OH}$. Regioisomeric 2-thienyl boronic acid (**3**) was found to undergo much faster protodeboronation (k_2 and $k_2$cat) than 3-thienyl **2**, with no significant disproportionation. In contrast, 2-furyl boronic acid (**4**, 1:1 d_8-dioxane/D_2O, 0.5 KOD; pD = pK_a) underwent disproportionation faster than protodeboronation when the concentration was raised to 0.4 M, Figure 3.

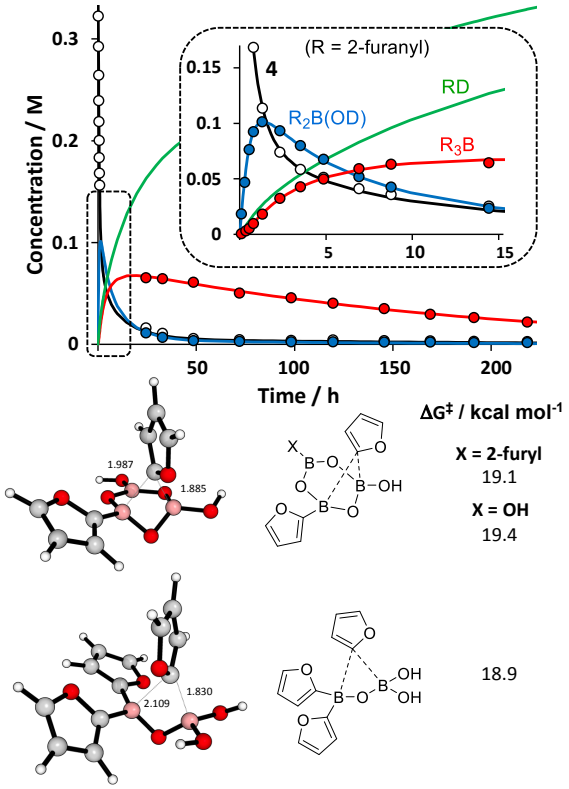

Figure 3. Upper: temporal concentration data for disproportionation of 2-furyl boronic acid **4** (1:1 d_8-dioxane/D_2O, 0.5 equiv. KOD, 70 °C). Circles: data. Solid lines: simulation (see SI for details). $^2H_1$-Furan (RD = **4**$_D$) is volatile under the reaction conditions and was not monitored. Lower: transition states (DFT) for disproportionation to difurylborinic acid and trifurylborane.[32]

The temporal evolution (^{1}H-NMR) indicated a two stage process, initially giving difurylborinic acid ($R_2B(OD)$), which disproportionates further to give the trifurylborane (R_3B, Figure 3). Over a period of days, all species protodeboronate, directly or indirectly, to give boric acid and furan (**4**$_D$).[33] DFT studies investigated a number of mechanisms for the aryl transfer between the boron centres. These included an analogue of autocatalysis mechanism, Figure 1, TS **2**$_{OH}$ (k_2*cat*), in which the furyl anion transfers to the Lewis acid B, rather than Bronsted acid H, in an H-bonded [**4**+**4**$_{OH}$] intermediate. However, the computed barrier for transfer to B (22.5 kcal/mol) is greater than for H (20.3 kcal/mol) and protodeboronation would dominate if solely these isomeric transition states are operative. An alternative process was therefore considered in which a cyclic boroxine-ate complex (Figure 3, X = furyl or OH, upper structure) facilitates aryl-migration across the ring. The rate-limiting barriers for aryl migration are computed to be 19.1-19.4 kcal/mol for 2-furyl **4**$_{OH}$ and 19.5-19.9 kcal/mol for 3-thienyl **2**$_{OH}$.

Accurately computing free energies in solution for very different processes is challenging, nonetheless, the calculations suggest that migration dominates over protodeboronation for 2-furyl **4**, while the opposite is the case for 3-thienyl **1**. The transition state structures suggest an electronic and steric component to this preference. Mulliken charges indicate the non-migrating 2-furyl bears a larger negative charge than the equivalent group for 3-thienyl. Further, the preferred conformation of the transition state places the migrating group in close proximity to the other aromatic ring; larger rings or those with C-H groups adjacent to the boronic acid group will, inevitably involve steric clashes, even more so when X = aryl. The subsequent step leading to triarylborane requires reaction of a borinic with a boronic acid and thus cannot involve a cyclic boroxine, is computed to proceed via a transition state involving a dimer (Figure 3, lower structure). The free energy barrier (+18.9 kcal/mol) is comparable to that for the first step, and thus consistent with the observed transient accumulation of diarylborinic acid. Using these models for reversible furyl transfer, with an irreversible protodeboronation, predominantly via the boronic acid, a good fit to the experimental data was achieved by kinetic simulation (solid lines, Figure 3).

4. General Model for Protodeboronation Kinetics. With suitable conditions established for analysis (50 mM substrate, 1:1 H_2O/1,4-dioxane, 70 °C) the pseudo first-order kinetics (k_{obs}) of reactions of boronic acids **2**-**19** were measured as a function of pH (1-13), Figure 4, Profiles **I**-**IV**, see SI for full details. Rates were pH dependent, and varied substantially between the boronic acids, with rate maxima that varied over 6 orders of magnitude (half-lives ranging from seconds to weeks). For some substrates, specific pH ranges reduced the protodeboronation rates to such an extent that, for reasons of accuracy, they were omitted from the log(k_{obs})-pH analyses. An arbitrary threshold of log k_{obs} ≥7.0 (half-life ≤80 days) was set for data inclusion (see dashed lines in profiles **I**-**IV**, Figure 4.

To analyse the pH-dependency of the protodeboronation reactions of heterocyclic boronic acids we developed a general model, Figure 5. Aiming to keep as minimal a model as required, we began with the Kuivila processes, and added further processes, when necessary, as the analysis of heterocyclic boronic acids **2**-**17** evolved. To simplify the discussion, the overarching model is presented in advance of the analysis of the protodeboronation characteristics of **2**-**17**. As many of the heterocyclic systems studied are basic, the model includes, when appropriate, the pK_{aH} of the *N*-protonated form of the heterocycle, in addition to the pK_a for aqueous association at boron.

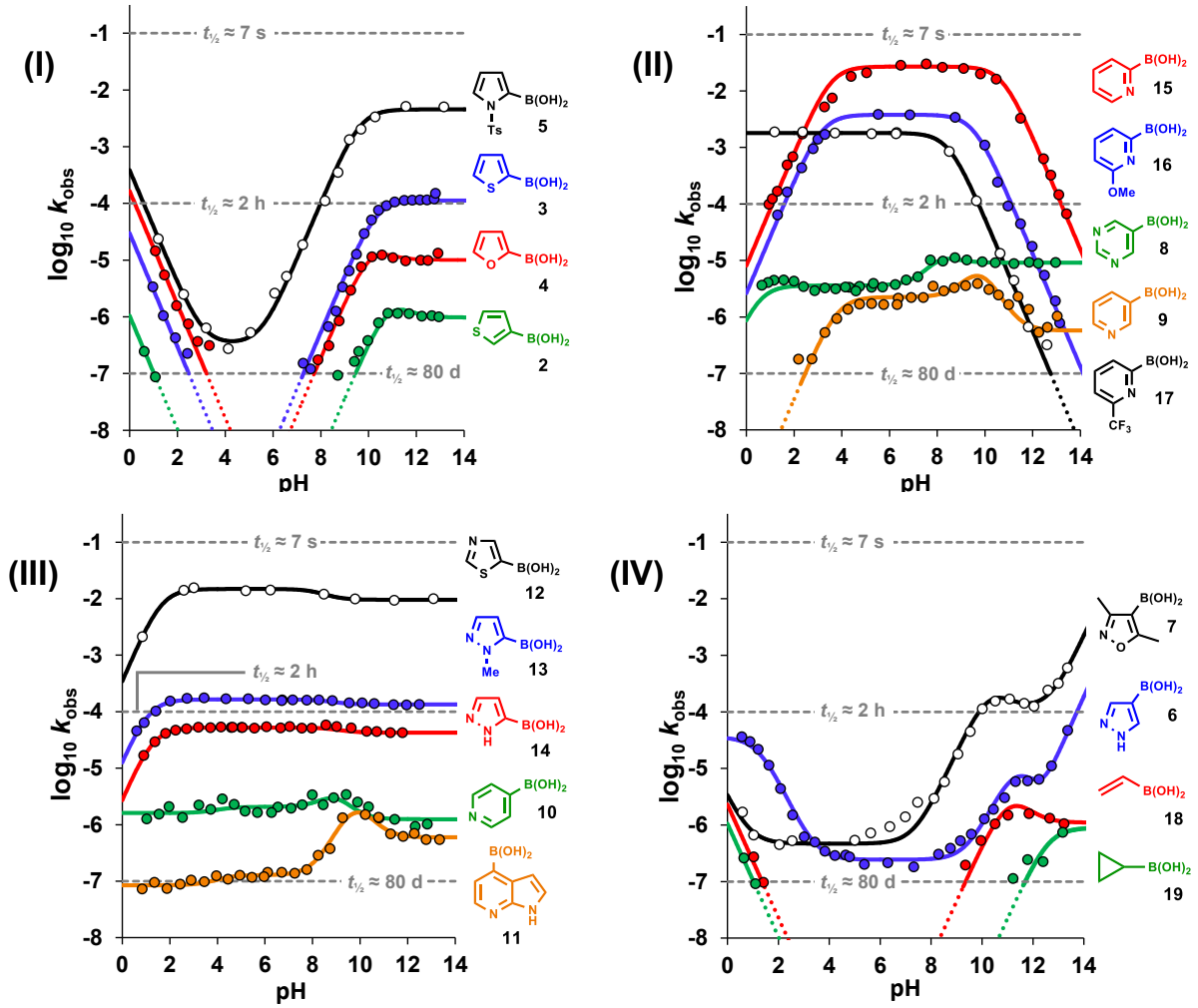

Figure 4. pH-rate profiles (**I-IV**) for pseudo first-order protodeboronation (k_{obs} / s^{-1}) of boronic acids **2–19** in 1:1 H_2O/1,4-dioxane at 70 °C. Reactions analysed *in situ* by ^{11}B NMR were conducted in quartz NMR tubes to avoid $[B(OH)_4]^-$ release from borosilicate NMR tubes. Circles: experimental data. Solid lines: simulation using General Model (Figure 5) with data from Table 2. Rates below logk_{obs} = -7 are not modelled.

The kinetics are determined by a three-fold speciation of the boronic acid ('**X**'): as an *N*-protonated form ($\mathbf{X}_{H+}$; only for **6-17**), a neutral form (**X**), and a boronate form ($\mathbf{X}_{OH}$). Specific protodeboronation processes occur from the three speciation states. For the neutral form (**X**), there is the acid-catalyzed Kuivala process (k_1), and a pH-independent direct reaction with water (k_4). For the latter, although this is not kinetically differentiated in the model, basic heterocyclic boronic acids can engage in a pre-equilbrium (K_4) with autoionized water to generate a zwitterionic adduct ($\mathbf{X}_{ZW}$). For the boronate form ($\mathbf{X}_{OH}$), there is the base-catalyzed Kuivala process (k_2), concentration-dependent auto-catalysis (k_2cat) occurring with rate maximum when pH = pK_a, and the Perrin mechanism involving base-catalyzed protonolyis (k_3). For the latter, although this is not kinetically differentiated in the model, the boronate can engage with hydroxide in a pre-equilbrium (K_3) to generate the dianion ($\mathbf{X}_O$). Finally, for the *N*-protonated form ($\mathbf{X}_{H+}$), this being distinct from the zwitterion ($\mathbf{X}_{ZW}$) due to the presence of a boronic acid not a boronate, there is a direct protodeboronation by water (k_5).

As indicated graphically beside the protodeboronation mechanisms in the model (Figure 5), each of the six processes (k_1, k_2, $k_2$cat, k_3, k_4, k_5) has a distinct pH-log k_{obs} profile. It can be instructive to consider hypothetical combinations of selected pH-log k_{obs} relationships; examples (***i***, ***ii*** and ***iii***) are pre-configured in the spreadsheet provided in the SI. By mathematically combining all six steps (see SI for full derivation) and calculating the three-state speciation an 'overall rate equation' (Figure 5, centre) can be generated. The equation allows analysis of the empirical rate (k_{obs}) as a function of pH and boronic acid concentration, using up to nine constants: pK_a, pK_{aH}, k_1, k'_2, k'_2cat, k'_3, k'_4, k'_5, pK_w, in which processes indicated by the term k', contain amalgamated constants (e.g. K, k and [H_2O]). For non-basic boronic acids, pK_{aH} is nominally set to -5 to preclude $\mathbf{X}_{H+}$ speciation.

Values for pK_a and pK_{aH} can be determined independently, or *via* the pH-log k_{obs} simulation. Initial pK_{aH} values for **6-17** were determined by ^1H NMR pH-titration (1:1 H_2O/1,4-dioxane, 25 °C), Table 2. An empirical correction for temperature (ΔpK_{aH} 25-70 °C = -0.46) was determined from the pH-rate profile simulation. Generally, the $B(OH)_2$ unit slightly decreases the basicity relative to the parent heterocycle.[34] For example, 2-, 3- and 4-pyridyl boronic acids (**15**, **9**, **10**) have pK_{aH} values (25 °C) of 3.86, 4.22, and 3.82, compared to that of 4.38 for pyridine, see SI. The pK_a values for most of the boronic acids were measured by ^{11}B NMR pH titration (1:1 H_2O/1,4-dioxane, 70 °C); the pK_a of the more reactive species (**5**, **12**, **15-17**) were estimated via the pH-log k_{obs} simulation.

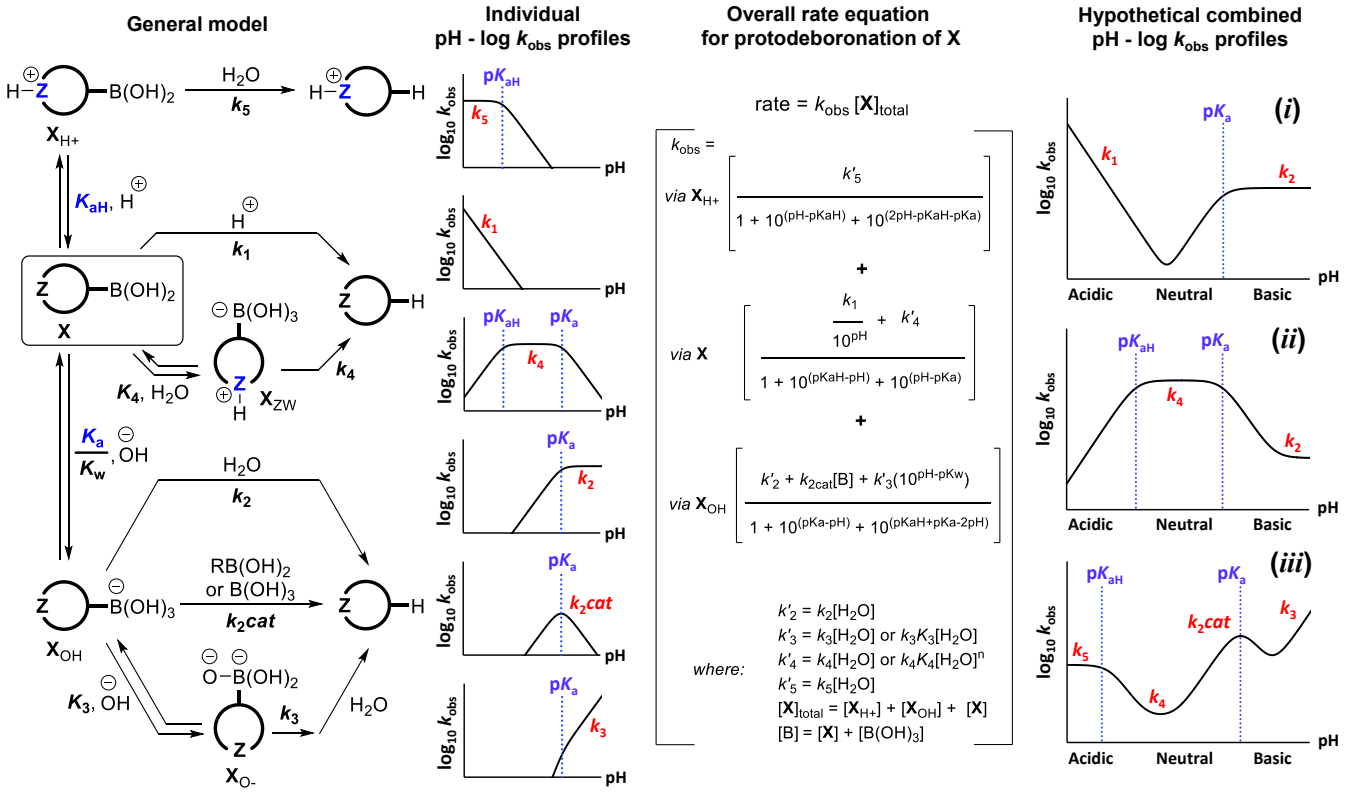

Figure 5. General model for heterocycle protodeboronation ('Z' = basic nitrogen), individual pH-log k_{obs} profiles, overall rate-equation based on the three-state speciation: neutral (**X**); *N*-protonated ($\mathbf{X}_{H+}$); and boronate ($\mathbf{X}_{OH}$), and example combined pH-log k_{obs} profiles (***i***, ***ii***, ***iii***).

5. pH-Rate Profiles Analysis of Boronic Acids 2-19. Using the rate equation in Figure 5, the pH-rate profiles for **2-19** were simulated by automated iteration of rate and equilibrium constants, minimizing the sum square error (SSE) between predicted and observed data across the full profile (pH 1 to 13). The SSE-minimized fitting constants are provided in Table 2. In all cases (**2-19**), only a sub-set of the six pathways (k_1, k_2', k_2cat, k_3', k_4', k'_5) were required for satisfactory simulation (solid lines through data, Figure 4). The constants that are not required for simulation, but are in principle feasible, are reported as threshold values (≤) that induce a ≥5% change in the SSE.[35]

Non-basic heterocycles (***2-5***). The thienyl (**2**,**3**) and furyl (**4**) boronic acids (Figure 4, profile **I**) required only the Kuivila-processes (k_1, k'_2)[17ck] and auto-catalysis ($k_2$cat) for simulation. The 2-pyrrole boronic acid **5** required an additional pH-independent process (k'_4),[21] to fit the data between pH 3-6. This process is slow enough (k'_4, half life >24 days) to be consistent with a water autoionization mechanism.[36] Higher reactivity of 2- versus 3-thienyl and furyl boronic acids has been noted before, but only for acid-catalysis (k_1).[22] In all cases (**2-5**), the base-catalyzed process (k'_2) is more efficient than the acid (k_1) and the rates rise substantially through the series; above pH 11, 2-pyrrolyl **5** has a half-life of less than 3 minutes.

Basic heterocycles (***6-17***). The rate data obtained for 2-pyridyl boronic acids **15-17** (profile **II**) show a near inverse pH-rate profile to the non-basic heterocycles **2-5** (profile **I**) and required just a single term (k'_4) for simulation. Maximum rates are attained when speciation *disfavours* the boronate (**15-17**$_{OH}$; high pH) and pyridinium (**15-17**$_{H+}$; low pH) forms. Thus for the least basic **17** (pK_{aH} <-0.6) the protodeboronation is not detectably attenuated by acid, even at pH 1. The much less reactive 5-pyrimidyl (**8**) and 3-pyridyl (**9**) systems required base-catalysis (k'_2 + $k_2$cat) in addition to the neutral mechanism (k'_4) for simulation. The 5-pyrazolyl and 5-thiazolyl boronic acids (**13-15**) were highly reactive, requiring both k'_4 (neutral) and k'_2 (basic) pathways for satisfactory simulation, with rates attenuated at pH below their pK_{aH}, (profile **III**). The 4-pyridyls (**10**, **11**) are of similar reactivity to 3-pyridyl (**9**), but differ in that they still protodeboronate effectively at a pH substantially below their pK_{aH} (profile **III**). This effect was satisfactorily simulated by including a direct (H_2O-mediated) protodeboronation of the conjugate acid (k'_5); the 4-pyridyl systems (**10**, **11**) were the only species requiring this. The two remaining basic heterocycles, 4-pyrazolyl (**6**) and 4-isoxazolyl (**7**), gave the most complex profiles, requiring acid (k_1), base (k'_2/k_{2cat}), base-catalyzed boronate (k'_3) and neutral (k'_4) pathways (profile **IV**; Figure 4). These were the only examples requiring the Perrin mechanism (k'_3), a process that in Ar-B(OH)$_2$ systems requires 2,6-disubstitution.[17k]

Vinyl and Cyclopropyl boronic acids (***18-19***). Strongly acidic or basic solutions were required to effect any significant protodeboronation of the vinyl (**18**) and cyclopropyl (**19**) boronic acids (profile **IV**). Even at pH ≥11 the half lives are weeks. A small selection of simple alkyl boronic acids (Me, *c*-Bu, and *c*-Hex) were also investigated. The extremely slow reactions (half-lives of months, see SI) made it difficult to clarify, by ^{1}H / ^{13}C / ^{11}B NMR analysis, if protodeboronation was the major pathway of decomposition, rather than, for example, oxidation.

Table 2. Equilibrium and rate constants employed in the pH simulation (see overall rate equation in Figure 5) for protodeboronation of heteroaromatic, vinyl and cyclopropyl boronic acids 2–19 in 1:1 H_2O/1,4-dioxane at 70 °C.

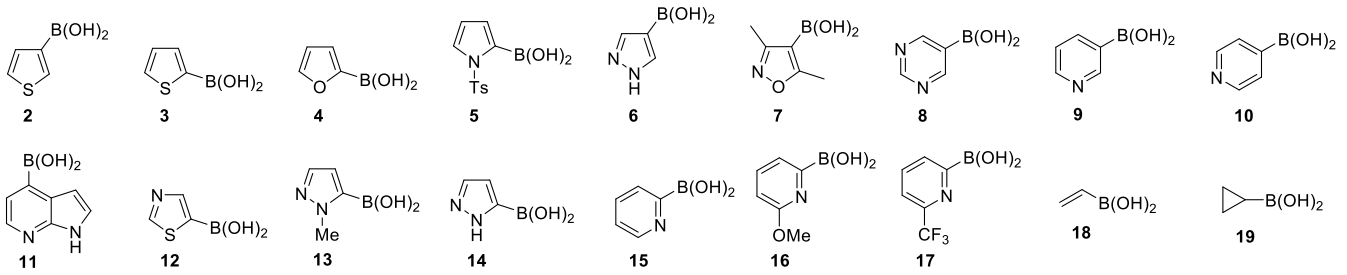

Entry	$RB(OH)_2$	pK_{aH}[a]	pK_a[b]	$\log k_1$	$\log k'_2$[c]	$\log k_{2cat}$	$\log k'_3$[e]	$\log k'_4$	$\log k'_5$
1	**2**	-	11.04	-5.95	-6.01	-4.21	≤-5.32[g]	-	-
2	**3**	-	10.38	-4.44	-3.92	≤-3.54	≤-3.07[g]	-	-
3	**4**	-	10.29	-3.71	-4.98	-3.32	≤-4.12[g]	-	-
4	**5**	-	9.64[c]	-3.41	-2.34	≤-2.07[d]	≤-1.93[d]	-6.48	-
5	**6**	1.26 (1.70)	11.61	-3.16	≤-6.02[d]	-3.27	-3.72	-6.60	≤-5.68[d]
6	**7**	0.04[e] (<0.50)	10.45	-5.51	-4.01	-2.00	-2.62	-6.38	≤-4.61[g]
7	**8**	0.14[e] (<0.60)	8.18	≤-4.82[d]	-5.04	-3.44	≤-4.75[d]	-5.44	≤-4.83[d]
8	**9**	3.60 (4.22)	9.76	≤-3.10[d]	-6.05	-3.60	≤-5.59[d]	-5.71	≤-6.70[d]
9	**10**	3.36[e] (3.82)	8.94	≤-3.76[d]	-5.93	-3.78	≤-5.78[d]	-5.71	-5.77
10	**11**	2.95[e] (3.41)	9.90	≤-5.64[d]	-6.24	-3.95	≤-6.60[d]	-6.89	-7.07
11	**12**	1.62 (1.85)	8.41[c]	≤-2.60[d]	-2.02	≤-1.58[d]	≤-2.21[d]	-1.83	≤-4.22[d]
12	**13**	1.08 (1.62)	8.82	≤-4.22[d]	-3.87	-3.49	≤-3.94[d]	-3.78	≤-5.31[d]
13	**14**	1.36 (2.00)	9.11	≤-4.58[d]	-4.35	-3.19	≤-3.93[d]	-4.28	≤-5.84[d]
14	**15**	3.52 (3.86)	10.76[c]	≤-0.74[d]	≤-4.26[d]	≤-0.67[d]	≤-3.74[d]	-1.60	≤-4.24[d]
15	**16**	3.16 (3.60)	9.54[c]	≤-1.36	≤-6.72[d]	≤-2.33[d]	≤-6.04[d]	-2.41	≤-4.52[d]
16	**17**	-1.06[e] (<-0.6)	8.49[c]	≤-2.06[d]	≤-6.32[d]	≤-1.84[d]	≤-4.82[d]	-2.75	≤-0.06[f]
17	**18**	-	11.21	-5.57	-6.02	-3.90	≤-5.73[d]	-	-
18	**19**	-	12.72	-5.95	-6.01	-5.01	≤-5.91[d]	-	-

a) pK_{aH} in parenthesis determined by ^{1}H-NMR pH titration at 25 °C; pK_{aH} at 70 °C from iterative fitting of rate data (unless stated); b) pK_a by ^{11}B-NMR pH titration at 70 °C (unless stated); c) pK_a from iterative fitting of rate data; d) this value is not required for satisfactory simulation; greater values induce ≥5% change in the sum of square errors between simulation and data across the overall pH profile; e) pK_{aH} fixed at empirical offset (-0.46 units) based on entries 5,8,11-16; f) due to the pK_{aH} of **17** being ≤1.06, this value is a substantial overestimate.

6. Protodeboronation Mechanisms for Basic Heterocycles. To aid rationalization of the diverse range of pH profiles for basic heterocycles **6-17**, protodeboronation mechanisms were explored by ^{11}B-NMR, DFT calculations (M06L/6-311++G**;[23] see SI for details), and by testing the effect of additives.

*Zwitterionic Water-Adducts (**17**$_{ZW}$).* 2-Pyridyl boronic acids are notorious for their susceptibility to protodeboronation,[1,8,11-13] as is found for **15-17**. However, only a single neutral process (k'_4) is required for simulation of the full pH-rate profile, indicating that the classic Kuivila-type acid and base catalyzed mechanisms (k_1 and k'_2) are negligible processes. Indeed H^+ / OH^- act as powerful protodeboronation inhibitors by modulating the speciation: the proportion of neutral boronic acid available for reaction by k'_4 is reduced by conversion to the protonated (**15-17**$_{H+}$) or boronate (**15-17**$_{OH}$) forms. Consequently, 2-pyridyl boronic acid **15** shows surprising stability at high pH (profile **II**, Figure 4) undergoing protodeboronation as slow, or slower, than many of the other heterocycles tested (e.g. **3-7**, **12-14**). The protodeboronation of **15-17** by water (k'_4) has a much lower energy barrier than the analogous protonation (k_2) of the boronate (**15-17**$_{OH}$). Irrespective of the likely contribution to direct hydrolysis by dynamic water fluctuation,[36] the free energy barriers calculated (DFT) for concerted aqueous cleavage of the C-B bond in neutral species **15-17** (47.9, 46.3 and 46.9 kcal/mol respectively) are far too high to account for the observed rates.

The ^{11}B NMR spectra of pyridyl species **15-17** in the pH region where maximum rate is attained (pH 4-8, Profile **II**, Figure 4) each display a *single* peak, arising from rapid equilibrium of the neutral boronic acid (**15-17**, approx. 28 ppm, broad) with a zwitterionic boronate **15-17**$_{ZW}$ (approx. 1 ppm, sharp). The zwitterionic species is formally generated by amphoteric capture of autoionized water (H^+, OH^-) at the Bronsted-basic and Lewis-

acidic (N, B) centres. At pH 6.5, the time-average chemical shifts, Figure 6, show that the equilibrium position between **15-17** and **15-17**$_{ZW}$ (K_4) is strongly modulated by the electron demand of the 6-substituent.

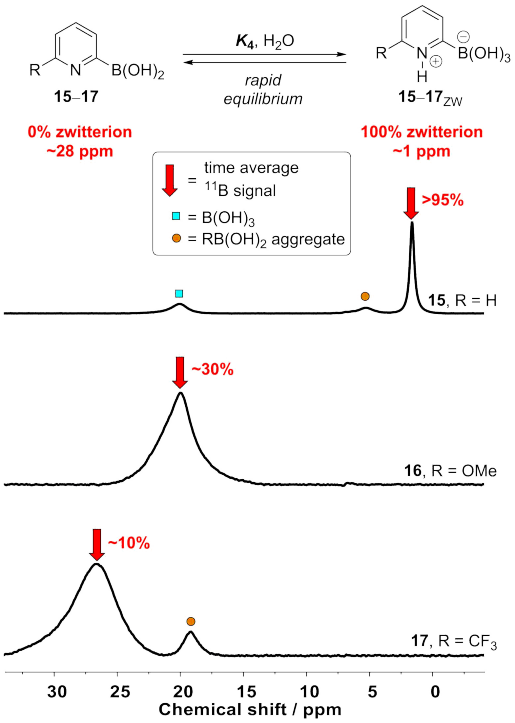

Figure 6. ^{11}B NMR spectra of 2-pyridyl boronic acids **15-17** (0.01 M, 25 °C) at pH 6.5 (AcO/AcOH buffer). Peaks correspond to time-average weighted chemical shifts between **15-17** (28 ppm, broad) and **15-17**$_{ZW}$ (1 ppm, sharp). Additional minor species are B(OH)$_3$ and aggregates, RB(OH)$_2$)$_n$, as indicated.

A key feature in all of the protodeboronations proceeding via fragmentation of zwitterionic water-adducts (k_4) is the intramolecular stabilization of the B(OH)$_3$ leaving group as C-B cleavage occurs. For the 2-pyridyl systems (e.g., TS **15**$_{ZW}$, k_4, Figure 7) this involves hydrogen-bonding with the positively charged pyridinium NH; in effect this solvates the B(OH)$_3$. However, this high reactivity (k_4) is not restricted to species with a protonated basic nitrogen atom *adjacent* to boron. Thiazolyl and pyrazolyl boronic acids (**12-14**), where the basic site is *remote* from boron, and for which water autoionization equilibria with zwitterionic species (**12-14**$_{ZW}$) is not detected (<10%) by ^{11}B NMR, also undergo rapid protodeboronation. DFT calculations support this observation: generation of the zwitterions (**12-14**$_{ZW}$) is much less favourable than for the pyridyl isomers **14-16**$_{ZW}$, but the transition states for their fragmentation, (TS **12-14**$_{ZW}$, k_4, Figure 7), are comparable in energy, due to other stabilizing interactions with the B(OH)$_3$ leaving group. For the thiazolium boronate (**12**$_{ZW}$, k_4), the anti-bonding orbital (C-Sσ*) acts as a surrogate H-bond, an extreme example of the interaction recently discussed by Meanwell.[37] For the pyrazolium systems (**13**, **14**), the highly polarized CH bond of the N-methyl (**13**$_{ZW}$, k_4) and NH (**14**$_{ZW}$, k_4) adjacent to NH$^+$ play the same stabilizing roles during heteroaryl-B(OH)$_3$ zwitterion fragmentation.

In the high pH region (pH > pK_a; 8.5-9.1) where the zwitterions (**12-14**$_{ZW}$) are converted to boronates (**12-14**$_{OH}$), the stabilizing interactions provided by C-Sσ*, CH and NH interactions, are still active, albeit attenuated (neutral basic N rather than NH$^+$). This attenuation is offset by the dominant boronate speciation, leading to only a small net reduction in protodeboronation rate (profile **III**, Figure 4). In contrast, for the pyridyl systems (**15-17**), the re-speciation to boronates **15-17**$_{OH}$ at high pH results in loss of the pyridinium NH stabilizing interaction, and a markedly different behaviour: the rate is strongly attenuated (profile **II**).

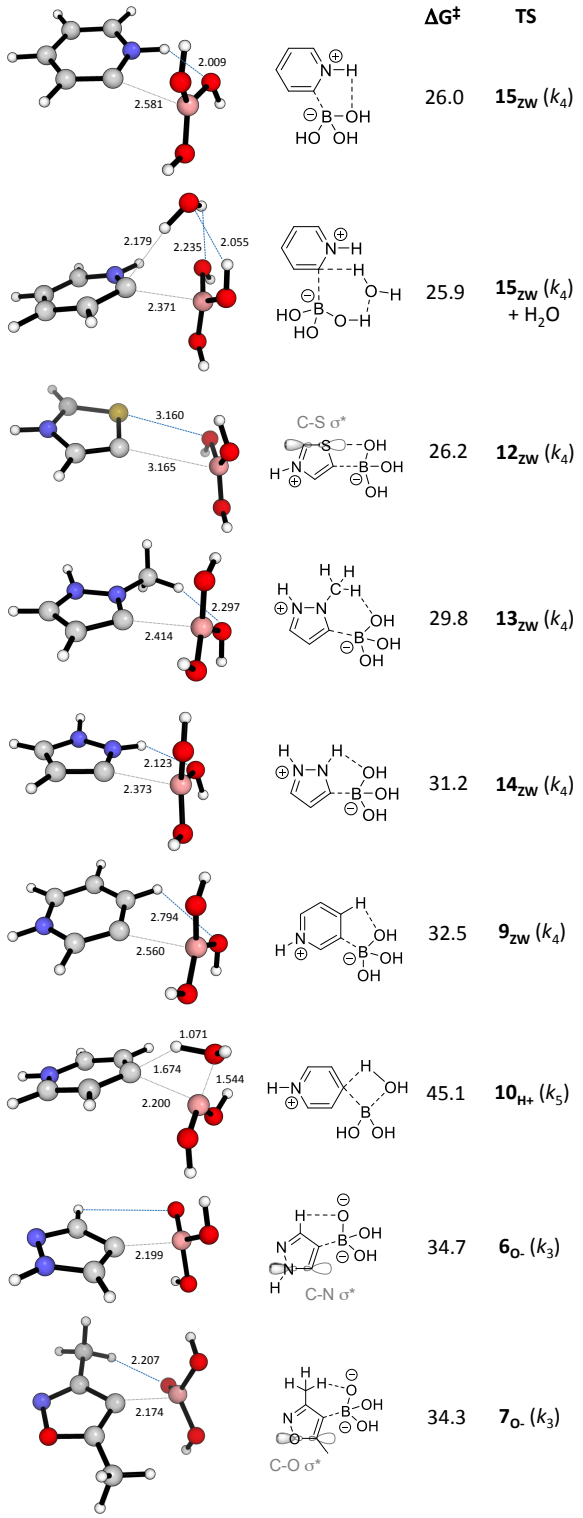

Figure 7. Selected transition state (TS) structures and calculated free energies (kcal/mol; M06L/6-311+G**)[23-27] for pathways k_4, k_5, and k_3, involving zwitterionic water adducts (**9**$_{ZW}$; **12**$_{ZW}$; **13**$_{ZW}$; **14**$_{ZW}$; **15**$_{ZW}$), pyridinium boronic acid (**10**$_{H+}$) and boronate dianions (**6**$_{O-}$ and **7**$_{O-}$) and respectively.

Equilibrium zwitterion populations are also low (^{11}B NMR; <10%) for 5-pyrimidyl (**8**), 3-pyridyl (**9**) and 4-pyridyl (**10**, **11**) boronic acids in neutral solution. This contrasts earlier reports where 3-and 4-pyridinium boronate zwitterions ($\mathbf{9}_{ZW}$ and $\mathbf{10}_{ZW}$) were concluded to be dominant (>90%) based on UV analysis of **9** and **10** in pure aqueous solution.[8d] DFT calculations suggest that not only are 3-pyridyl $\mathbf{9}_{ZW}$ and 4-pyridyl $\mathbf{10}_{ZW}$ higher in energy than 2-pyridyl $\mathbf{15}_{ZW}$, but also that the greater charge separation, lack of ylidic character[38] and poorer stabilization of the departing $B(OH)_3$ in the fragmentation (k_4), reduce their reactivity compared to **15**-**17**. The approximately 6 kcal/mol higher barriers for fragmentation, near-quantitatively predict the four orders of magnitude slower reaction, e.g. compare 3-pyridyl-$\mathbf{9}_{ZW}$, k_4 with 2-pyridyl-$\mathbf{15}_{ZW}$, k_4, Figure 7.

Protodeboronation at 4-Pyridinium (k_5) Despite 3-pyridyl (**9**) and 4-pyridyl (**10**) boronic acids undergoing protodeboronation via zwitterionic intermediates ($\mathbf{9}_{ZW}$ and $\mathbf{10}_{ZW}$) at similar rates, there is a key difference between their pH-rate profiles (see profiles **II** and **III**, Figure 4). For the 3-pyridyl system (**9**) the rate is strongly attenuated when the pH approaches and goes below pK_{aH} (3.60) due to re-speciation of the neutral **9**/**9** $_{ZW}$ form to $\mathbf{9}_{H+}$, where the N is fully protonated and the B-centre is boronic acid not boronate. In contrast, the 4-pyridyl boronic acids (**10**, **11**) display near-constant k_{obs} as the pH migrates through and below the pK_{aH} (3.36 and 2.95) indicative that the pyridinium species ($\mathbf{10}_{H+}$, $\mathbf{11}_{H+}$) are also reactive components. A mechanism involving attack at the boron in pyridinium $\mathbf{10}_{H+}$ by water to access a dipolar-carbene[38,39] intermediate is supported by DFT studies, Figure 7. The barrier for this process ($\mathbf{10}_{H+}$ / k_5; Figure 7) whilst high, is close to that computed for the normal protodeboronation under neutral conditions.

Boronate Deprotonation (k'_3) As noted above, k'_3, a mechanism in which base catalyzes the decomposition of the boronate, was required for kinetic simulation of 4-pyrazolyl (**6**) and 4-isoxazolyl (**7**) boronic acids at high pH. The Perrin mechanism (k'_3) has previously only been found in aryl systems bearing 2,6-disubstitution.[17k,39] The data, obtained at pH 12-13 (profile **IV**, Figure 4), the upper limit of the pH range attainable whilst retaining homogeneous reactions, confirm the first-order dependence on $[OH]^-$ and on boronate ($\mathbf{6}_{OH}$/$\mathbf{7}_{OH}$) - i.e. an increase (gradient +1.0) of log k_{obs} with pH, *after* the k_2-plateau. In principle, if boronate deprotonation is at equilibrium, a second pH rate plateau will be reached (at much higher pH than explored) after boronates $\mathbf{6}_{OH}$/$\mathbf{7}_{OH}$ are fully converted to $\mathbf{6}_{O}$/$\mathbf{7}_{O}$.

DFT calculations[23] suggest that protodeboronation via k'_3 requires the heterocycle to be able to stabilize *both* the deprotonated boronate ($\mathbf{6}_{O}$/$\mathbf{7}_{O}$) and the carbanion arising from its C-B fragmentation (k_3). The 4-pyrazolyl ring (TS $\mathbf{6}_{O}$, k_3; Figure 7) facilitates this stabilization using the adjacent C-Nσ^* orbital; an analogous C-Oσ^* orbital is available with the 3-isoxazolyl ring (TS $\mathbf{7}_{O}$, k_3; Figure 7) (**6**). In contrast, although a 5-pyrazolyl ring ($\mathbf{14}_{O}$) can stabilize the boronate by interaction with the adjacent NH, it cannot provide stabilization of a *carbanion* arising by C-B fragmentation. As a consequence, at high pH the protodeboronation rates of **6** and **7**, but not **14**, rise as the concentration of [OH] becomes sufficient to deprotonate the corresponding boronates.

Bis-boronate Protolysis (k'_2-mono and k'_2-bis). Prompted by the problems caused by protodeboronation when bis-boryl species are employed in co-polymerization cross-couplings under basic conditions,[40] we also determined the protodeboronation kinetics of a bis-boronic acid. The rates provide information on the intramolecular effect of one boronic acid on the reactivity of another. Choosing a simple 2,5-thienyl substrate, **20**, we simulated the kinetics using a model (Figure 8) in which there are two aqueous association constants (K_a-*mono* and K_a-*bis*) and two protonolysis rates (k'_2-*mono* and k'_2-*bis*) for the resulting boronates ($\mathbf{20}_{OH}$-*mono* and $\mathbf{20}_{OH}$*bis*). From this data, it can be seen that $\mathbf{20}_{OH}$*mono* reacts two-fold faster than the 2-thienyl-boronate $\mathbf{3}_{OH}$, in other words the presence of the spectator boronic acid in $\mathbf{20}_{OH}$*mono* has a small impact on the rate, and slightly increases the Lewis acidity at boron (pK_a = 9.5). In contrast, $\mathbf{20}_{OH}$*bis* is about eight-fold less reactive than $\mathbf{20}_{OH}$*mono*, when statistically normalized, indicating that the boronate group induces mild rate-suppression, and substantially decreases the Lewis acidity at boron (pK_a = 11.6). As such, using media at a higher than usual pH may be of benefit in polymerization cross-couplings of bis-boryl species.

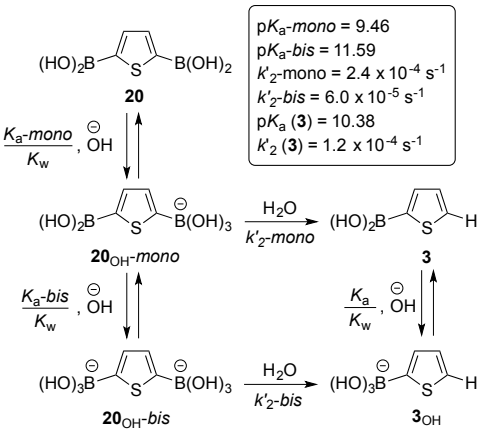

Figure 8. Rate comparison protodeboronation of 2,5-bis-boronyl thiophene **20** and 2- boronyl thiophene **3** in the range pH 6-13 (50 mM, 1:1 dioxane/H_2O, 70 °C), rate and equilibrium constants obtained by pH-rate profile simulation, pH 6-13, see SI.

7. The Effect of Additives (Cu, Zn, B) on Protodeboronation. In addition to identification of the zwitterionic water adduct ($\mathbf{15}_{ZW}$) for of 2-pyridyl boronic acid by ^{11}B NMR, analysis at various concentrations revealed the presence of aggregates, $(\mathbf{15})_n$ ($\delta_B \approx 6$ ppm, see Figure 6). Analysis of the protodeboronation kinetics at various concentrations revealed that generation of aggregates reduce the proportion of zwitterion generated, resulting in mildly attenuated protodeboronation rates, compare entries A and B, Table 3. The pseudo first-order kinetics obtained in these protodeboronation reactions indicate that the boric acid co-product also attenuates protodeboronation, as confirmed by reaction of **15,** 0.05 M, in the presence of added boric acid, 0.15 M, entry C. Other Lewis acid additives ($MgCl_2$, $Sc(OTf)_3$, $ZnCl_2$, and $CuCl_2$; entries D-G) were tested, of which $CuCl_2$, the most azaphilic, had the greatest impact, increasing the half life of **15** by a factor of 24.

Analysis of this process (entry G) *in situ* by NMR was not informative due to the paramagnetic Cu(II). However, addition of 2,2'-bipyridine *during* a $CuCl_2$-attenuated protodeboronation (entry H, Figure 9) resulted in reinstatement of rapid protodeboronation, through competition of **15** and 2,2'- bipyridine for the Cu. Thus, irreversible transmetallation (Cu for B) is not responsible for the protodeboronation rate suppression.

Table 3. The effect of additives on the protodeboronation kinetics of 12-15 at pH 6.2-6.9 in 1:1 H_2O/1,4-dioxane at 70 °C.

Entry	[RB(OH)$_2$]	Additive (conc.)	k_{obs} 10^3/ s^{-1}	$t_{½}$
A	**15**, 0.05 M	-	27.9	25 s
B	**15**, 0.20 M	-	20.8	33 s
C	**15**, 0.05 M	B(OH)$_3$ (0.15 M)	20.0	34 s
D	**15**, 0.05 M	$MgCl_2$ (0.10 M)	28.8	24 s
E	**15**, 0.05 M	Sc(OTf)$_3$ (0.10 M)	12.9	53 s
F	**15**, 0.05 M	$ZnCl_2$ (0.10 M)	8.4	82 s
G	**15**, 0.05 M	$CuCl_2$ (0.10 M)	1.20	10 min
H	**15**, 0.05 M	$CuCl_2$ (0.10 M)[a]	16.9	41 s[a]
I	**12**, 0.05 M	-	14.4	48 s
J	**12**, 0.05 M	$ZnCl_2$ (0.10 M)	50.5	14 s
K	**13**, 0.05 M	-	0.184	63 min
L	**13**, 0.05 M	$ZnCl_2$ (0.10 M)	2.20	5 min
M	**14**, 0.05 M	-	0.068	169 min
N	**14**, 0.05 M	$ZnCl_2$ (0.10 M)	0.902	13 min

[a] bipy (0.2 M) added at 80 seconds

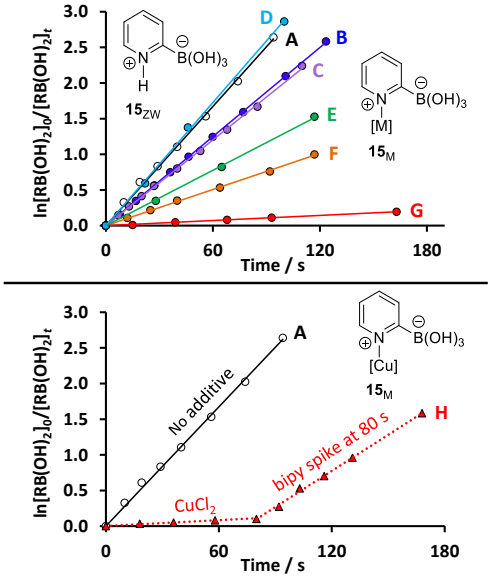

Figure 9. Pseudo first-order protodeboronation kinetics for **15** in the presence of Lewis acid additives.

^{11}B NMR analysis of the reaction of **15** containing a $ZnCl_2$ additive[13c] (entry F) indicated that a boronate is still present (δ_B 1.5 ppm). The inhibiting effect thus arises from reversible pyridine complexation (**15**$_M$; M = Zn, Cu etc.), reducing the proportion of zwitterion (**15**$_{ZW}$) available for fragmentation (k_4). As noted above, the 5-thiazolium system undergoes rapid protodeboronation (**12**$_{OH}$ k'_4; and **12**$_{ZW}$ k'_4, Figure 7) through C-Sσ* stabilization of the TS for fragmentation. Thus, unlike the 2-pyridyl system **15**, which relies on stabilization by the adjacent NH+, metal-complexation at the 5-thiazolium nitrogen (**12**$_M$) does not negate the stabilization, but in contrast exacerbates the effect of the C-Sσ*, resulting in even faster protodeboronation (entries I,J, Figure 10). The same effects are found for **13** and **14**, where *N*-complexation by [Zn] augments the boronate stabilizing effect of the N-methyl (**13**$_M$) and NH (**14**$_M$) groups, resulting in more rapid protodeboronation (Table 3, entries K-N, Figure 10).

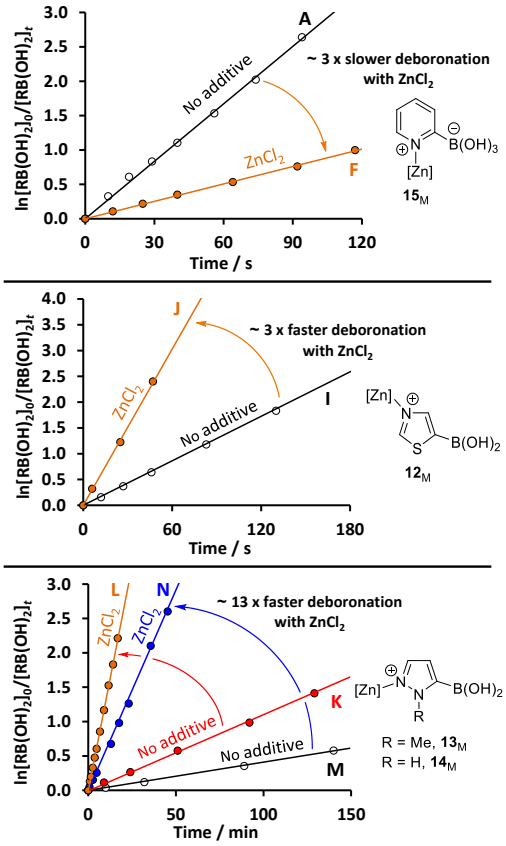

Figure 10. The effect of 2 equiv. $ZnCl_2$ on protodeboronation of **12-15** in 1:1 H_2O/1,4-dioxane, 70 °C, pH 6.2-6.9 (NaOAc/AcOH).

Conclusions

As summarised in Figure 11, and contrary to general perception, many heterocyclic systems, including **2-5** and **8-11**, undergo very slow aqueous protodeboronation, even at very high pH. Large stoichiometric excess can often be required for the successful Suzuki-Miyaura coupling of vinyl (**18**) and cyclopropyl (**19**) boronic acids. The resistance of **18** and **19** to protodeboronation (half-lives of weeks) suggest that the cross-coupling conditions,[19] rather than intrinsinc reagent instability, that causes this. Nonetheless, some heterocyclic boronic acids, e.g. **6**, **7**, **12-17**, can undergo rapid protodeboronation, but only in specific pH ranges. In all of these cases rapid protodeboronation is facilitated by stabilization of the B(OH)$_3$ during C-B fragmentation. For the 2-pyridyl system, this stabilization is provided by the pyridinium NH in a zwitterion (**15-17**$_{ZW}$), in **12** it is provided by an adjacent C-Sσ*, and in **13**, **14** by an adjacent polarized NMe or NH. Additional stablization of the carbanion arising from C-B fragmentation (k_3) is provided in 5-pyrazolyl and 5-isoxazolyl systems by adjacent C-Nσ* (**6**) and C-Nσ* (**7**) orbitals. *N*-alkylation, e.g. to generate methyl pyridinium boronates,[41] will reduce pK_a, making k_2 accessible at a lower pH. *N*-methylation may also effect stabilization of B(OH)$_3$ during 2-pyridyl C-B fragmentation by interaction with the highly polarized N-CH$_3$ unit, analogous to that in **13**$_{ZW}$, k_4, Figure 7.

A key aspect in all of the reactive systems studied (**6**, **7**, **12-17**) is that the pH controls the speciation of the boronic acid ('**X**') between various protonated, neutral, boronate and deprotonated states (**X**$_{H+}$, **X**$_{ZW}$, **X**, **X**$_{OH}$, and **X**$_O$). The speciation regulates which specific protodeboronation processes (k_1, k_2, k_2cat, k_3, k_4, k_5) are available, and thus governs the overall rate.

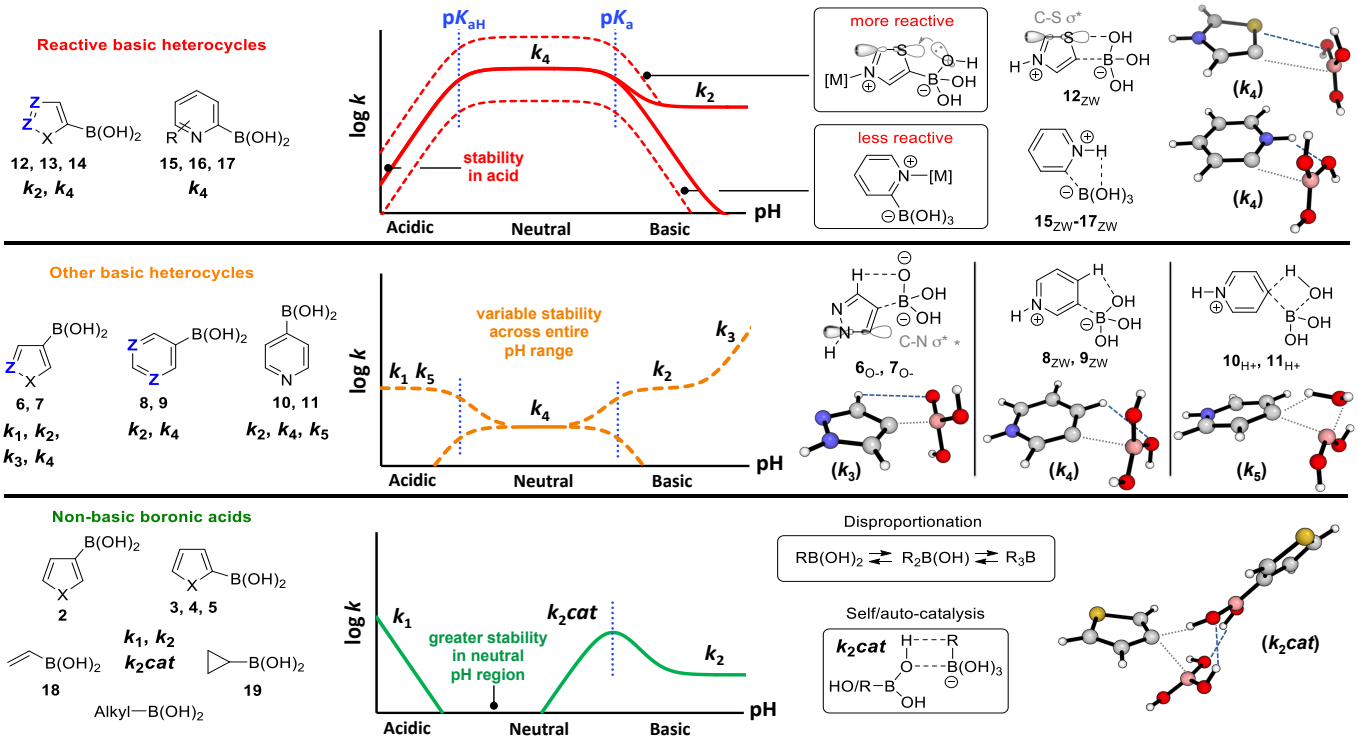

Figure 11. Schematic relationships for protodeboronation rate (log k_{obs}) and pH (arbitrary scale - refer to **I-IV**, Figure 4) allowing classification of boronic acids according to the impact of basic sites (Z = N_{Ar}), antibonding orbitals, and effect of added Lewis acids (MX_n). In structures where more than one Z is indicated, only one site need be basic (i.e. N_{Ar}), the remainder can also be CH, CR, CX, etc.

For example, 2-pyridyl-boronic acid (**15**) has a half-life of ≥ 2 hours at pH 1 (as $\mathbf{15}_{H+}$) or at pH 13 (as $\mathbf{15}_{OH}$) but just 26 seconds between pH 4-10 because maximum $\mathbf{15}_{ZW}$ is available for pathway k_4. Electron withdrawing groups in the 6-position (**16**, **17**) reduce both pK_{aH} and pK_a, resulting in the high-reactivity being expressed in a lower pH range. In contrast to 2-pyridyl-**15**, 5-thiazolyl, and 5-pyrazolyl boronic acids are reactive in both the zwitterionic (**12-14**$_{ZW}$, k_4) and boronate (**12-14**$_{OH}$, k_2) forms, leading to a much wider pH range for fast protodeboronation (compare profiles **II** and **III**, Figure 4).

When high concentrations of boronic acid *and* boronate are present, bimolecular processes can occur, resulting in protodeboronation auto-catalysis ($k_2$cat, Figures 1 and 2) and disproportionation (Figure 3). Whilst borinic ($R_2B(OH)$) and borane (R_3B) reagents have been employed in Suzuki-Miyaura couplings,[42] their different reactivity may lead to more complex reaction profiles. The slow release[9a,11a] of boronic acids from MIDA boronates,[8a,9a,15] or trifluoroborates,[16] maintains low $RB(OH)_2$ concentrations, and can thus reduce competing bimolecular auto-catalysis and disproportionation. This will be most important in the range pH = pK_a ± 1.6, where the speciation allows co-existence[43] of boronic acid *and* boronate.

Lewis acid additives (Table 3, Figures 9,10) can exacerbate or attenuate protodeboronation of basic heterocycles, across the whole pH range. For the 2-pyridyl systems, protodeboronation rates are reduced by lowering the zwitterion concentration (**15-17**$_{ZW}$, k_4). This may partially explain the beneficial effect of additives, such as copper salts, in the coupling of 2-pyridyl boronic acids.[8c,13] However, Lewis acids have the opposite effect for **12-14**, where complexation to the remote basic nitrogen augments boronate stabilization (by C-Sσ*, NMe and NH) at the fragmentation TS (k_2 / k_3) thus accelerating protodeboronation.

Our kinetic studies (Tables 1 and 2) also provide insight to other protodeboronation reactions. For example, Perrin found *p*-anisyl boronic acid (**1**) to equilibrate instantly with the corresponding trifluoroborate ($ArBF_3K$) in aqueous HCl / KHF_2 (pH 2), with protodeboronation to generate $\mathbf{1}_H$ occurring with a half life of less than 3 minutes. At pH 2, the half-life of **1** is 11 hours at 90 °C (k_1, Table 1, entry 1). Clearly the protodeboronation proceeds *directly* from the trifluoroborate, as was suggested by Perrin.[17k] In contrast to **1**, where the concentration of the trihydroxyboronate form ($\mathbf{1}_{OH}$) is vanishingly low at low pH, the trifluoroborate form $ArBF_3K$ is stable under these conditions (pH 2) and C-B protonolysis (k_2, H^+) is anticipated to be fast. On this basis, 2-pyridyl trifluoroborates are also expected to readily protodeboronate, as reported by Molander.[44]

In summary Heteroaromatic boronic acids **2-17** undergo protodeboronation in 1:1 dioxane/H_2O at 70 °C with a diverse range of rates and pH profiles (Figure 2, Figure 4). Whilst there is *no overall trend* in terms of reactivity or specific pH zones for highest stability: each class of heteroaromatic boronic acid (Figure 11) can be evaluated for likely speciation at a given pH, and factors that induce instability identified. These factors include: i) a basic nitrogen centre that allows zwitterion generation by reaction with autoionized water; ii) an N-H, X-H, or polarized NC-H group adjacent to the boronate to interact and stabilize it during C-B fragmentation; and iii) an adjacent antibonding orbital (C-Xσ*, X = S,N,O) that can overlap with the carbanion formally generated during C-B fragmentation.

ASSOCIATED CONTENT

Supporting Information: kinetic data, simulation, synthesis, characterization and NMR spectra.

AUTHOR INFORMATION

Corresponding Author: Guy.lloyd-jones@ed.ac.uk

Notes The authors declare no competing financial interest

Contributions The manuscript was written by all authors.

Funding Sources The research leading to these results has received funding from the European Research Council under the European Union's Seventh Framework Programme (FP7/2007-2013) / ERC grant agreement n° [340163].

ACKNOWLEDGMENT

We thank Craig P. Butts, Juraj Bella and Lorna Murray for NMR assistance. AGL thanks the NSCCS for computational support and Gary Noonan for useful discussions.

REFERENCES

(1) Hall, D, (Ed); *Boronic acids: preparation and applications in organic synthesis, medicine and materials (vols 1 and 2),* Second edition, **2011**, pp 1-133, Wiley VCH, Weineheim, Germany.

(2) (a) Miyaura, N.; Yamada, K.; Suzuki, A. *Tetrahedron Lett.* **1979**, *20*, 3437-3440; (b) Miyaura, N.; Suzuki, A. *Chem. Rev.* **1995**, *95*, 2457-2483.

(3) Cho, C. S.; Uemura, S. *J. Organomet. Chem.* **1994**, *465*, 85-92.

(4) (a) Chan, D. M. T.; Monaco, K. L.; Wang, R.-P. P.; Winters, M. P. *Tetrahedron Lett.* **1998**, *39*, 2933-2936; (b) Evans, D. A.; Katz, J. L.; West, T. R. *Tetrahedron Lett.* **1998**, *39*, 2937-2940; (c) Lam, P. Y. S.; Clark, C. G.; Saubern, S.; Adams, J.; Winters, M. P.; Chan, D. M. T.; Combs, A. *Tetrahedron Lett.* **1998**, *39*, 2941-2944.

(5) Liebeskind, L. S.; Srogl, J. *J. Am. Chem. Soc.* **2000**, *122*, 11260-11261.

(6) (a) Sakai, M.; Hayashi, H.; Miyaura, N. *Organometallics* **1997**, *16*, 4229-4231; (b) Cho, C. S.; Motofusa, S.; Ohe, K.; Uemura, S.; Shim, S. C. *J. Org. Chem.* **1995**, *60*, 883-888.

(7) (a) Sakai, M.; Ueda, M.; Miyaura, N. *Angew. Chem. Int. Ed.* **1998**, *37*, 3279-3281; (b) Takezawa, A.; Yamaguchi, K.; Ohmura, T.; Yamamoto, Y.; Miyaura, N. *Synlett* **2002**, *10*, 1733-1735.

(8) (a) Review: Tyrrell, E.; Brookes, P. *Synthesis* **2003**, *4*, 469-483; (b) Ishiyama, T.; Ishida, K.; Miyaura, N. *Tetrahedron* **2001**, *57*, 9813-9816; (c) Dick, G. R., Woerly, E. M., Burke, M. D. *Angew. Chem. Int. Ed.* **2012,** *51,* 2667-2672; (d) Fischer, F. C.; Havinga, E. *Recl. des Trav. Chim. des Pays-Bas* **1974**, *93*, 21.

(9) (a) Knapp, D. M.; Gillis, E. P.; Burke, M. D. *J. Am. Chem. Soc.* **2009**, *131*, 6961-6963; (b) Matteson, D. S. *J. Am. Chem. Soc.* **1960**, *82*, 4228; (c) Peyroux, E.; Berthiol, F.; Doucet, H.; Santelli, M. *Eur. J. Org. Chem.* **2004**, *5*, 1075-1082; (d) Denmark, S. E.; Butler, C. R. *Chem. Commun.* **2009**, *1*, 20-33.

(10) (a) Molander, G. A.; Gormisky, P. E. *J. Org. Chem.* **2008**, *73*, 7481-7485; (b) Lemhadri, M.; Doucet, H.; Santelli, M. *Synth. Commun.* **2006**, *36*, 121-128; (c) Wallace, D. J.; Chen, C. *Tetrahedron Lett.* **2002**, *43*, 6987-6990; (d) Zhou, S.-M.; Deng, M.-Z.; Xia, L.-J.; Tang, M.-H. *Angew. Chem. Int. Ed.* **1998**, *37*, 2845-2847; (e) Chen, X.; Goodhue, C. E.; Yu, J. Q. *J. Am. Chem. Soc.* **2006**, *128*, 12634-12635; (f) Chen, H.; Deng, M.-Z. *Org. Lett.* **2000**, *2*, 1649-1651; (g) Fang, G. H.; Yan, Z. J.; Deng, M. Z. *Org. Lett.* **2004**, *6*, 357-360.

(11) (a) Lennox, A. J. J.; Lloyd-Jones, G. C. *Isr. J. Chem.* **2010**, *50*, 664-674; (b) Lennox, A. J. J.; Lloyd-Jones, G. C. *Chem. Soc. Rev.* **2014**, *43*, 412-443.

(12) Kinzel, T.; Zhang, Y.; Buchwald, S. L. *J. Am. Chem. Soc.* **2010**, *132*, 14073-14075.

(13) (a) Deng, J. Z.; Paone, D. V.; Ginnetti, A. T.; Kurihara, H.; Dreher, S. D.; Weissman, S. A.; Stauffer, S. R.; Burgey, C. S. *Org. Lett.* **2009**, *11*, 345-347; (b) Chen, J.; Cammers-Goodwin, A. *Tetrahedron Lett.* **2003**, *44*, 1503-1506; (c) Chen, K., Peterson, R., Math, S.K., LaMunyon, J. B., Testa, C.A., Cefalo, D.R., *Tetrahedron Lett.*, **2012**, *53*, 4873–4876.

(14) Robbins, D. W.; Hartwig, J. F. *Org. Lett.* **2012**, *14*, 4266-4269.

(15) Li, J.; Grillo, A. S.; Burke, M. D. *Acc. Chem. Res.* **2015,** *48*, 2297–2307.

(16) (a) Molander, G. A. *J. Org. Chem.* **2015**, *80*, 7837-7848; (b) Butters, M.; Harvey, J. N.; Jover, J.; Lennox, A. J. J.; Lloyd-Jones, G. C.; Murray, P. M. *Angew. Chem. Int. Ed.* **2010**, *49*, 5156-5160; (c) see reference 29 in: Lennox, A. J. J.; Lloyd-Jones, G. C. *J. Am. Chem. Soc.* **2012**, *134*, 7431-7441.

(17) (a) Ainsley A. D.; Challenger, F. *J. Am. Chem. Soc.* **1930**, *52*, 2171-2180; (b) Johnson, J.R., Van Campen, M.G., Jr., Grummit, O. *J. Am. Chem. Soc.* **1938**, *60*, 111-115; (c) Kuivila, H. G.; Nahabedian, K. V. *J. Am. Chem. Soc.* **1961**, *83*, 2159-2163; (d) Kuivila, H. G.; Nahabedian, K. V. *J. Am. Chem. Soc.* **1961**, *83*, 2164-2166; (e) Nahabedian, K. V; Kuivila, H. G. *J. Am. Chem. Soc.* **1961**, *83*, 2167-2174; (f) Kuivila, H. G.; Reuwer, J. F.; Mangravite, J. A. *Can. J. Chem.* **1963**, *41*, 3081-3090; (g) Kuivila, H. G.; Reuwer, J. F.; Mangravite, J. A. *J. Am. Chem. Soc.* **1964**, *86*, 2666-2670; (h) Beckett, M. A.; Gilmore, R. J.; Idrees, K. *J. Organometal. Chem.* **1993**, *455*, 47-49; (i) Frohn, H.-J.; Adonin, N. Y.; Bardin, V. V.; Starichenko, V. F. *Z. Anorg. Allg. Chem.* **2002**, *628*, 2834-2838; (j) Cammidge, A. N.; Crepy, K. V. L. *J. Org. Chem.* **2003**, *68*, 6832-6835.; (k) Lozada, J.; Liu, Z.; Perrin, D. M. *J. Org. Chem.* **2014**, *79*, 5365-5368; (l) Noonan, G.; Leach, A. G. *Org. Biomol. Chem.* **2015**, *13*, 2555-2560;

(18) K_a is the equilibrium of $RB(OH)_2$ with $[RB(OH)_3^-][H^+]$ and is distinct from K_{aH}, the N-protonation of basic heterocycles.

(19) see e.g. a) Kallepalli, V. A., Gore, K. A. Shi, F., Sanchez, L., Chotana, G. A., Miller, S. L. Maleczka, Jr., R. E., Smith, III

M. R. *J. Org. Chem.*, **2015**, *80*, 8341-8353; b) Barker,G., Webster, S., Johnson, D. G., Curley, R., Andrews, M., Young, P. C., Macgregor, S. A., Lee. A.-L. *J. Org. Chem.*, **2015**, *80*, 9807-9816.

(20) The autoionization (*Kw*) of water, pH, p*Ka* of $RB(OH)_2$, and pK_{aH} of a protonated centre (e.g., heterocycle) changes with temperature. Changing from H_2O to H_2O/dioxane 50/50 induces ΔpKa +1 and ΔpK_{aH} -1. See SI for discussion of *Kw*.

(21) Kuivila noted a slow, pH-independent, hydrolysis of 2,-6-dimethoxyphenyl boronic acid.[17f] In our studies, capricious background hydrolysis occured at neutral pH with some substrates, e.g. **1** and **2**. This process was fully supressed by addition of small amounts of chloride ion, suggesting catalysis by trace metal impurities. For systems where k_4 was a required mechanism (e.g. **5**, **12-17**) rates were unaffected by added chloride.

(22) (a) Brown, R. D.; Buchanan, A. S.; Humffray, A. A. *Aust. J. Chem.* **1965**, *18*, 1521-1525; (b) Deans, F. B.; Eaborn, C. *J. Chem. Soc.* **1959**, 2303-2318; (c) Florentin, D.; Fournie-Zaluski, M. C.; Callanquin, M.; Roques, B. P. J. Heterocycl. Chem. 1976, 13, 1265–1272.

(23) a) M06L/6-311++G**, incorporating solvation free-energies computed as single points employing the same level of theory and the PCM formalism;[24] this level gave best quantitative agreement with experiment for MIDA hydrolysis.[5] b) M06/6-311+G**//B3LYP/6-31+G**, was used for selected species, incorporating solvation via a single point using B3LYP/6-31+G* combined with the PCM formalism as implemented in Gaussian03;[26] this level was previously used for boronic acids.[17l,27] Calculations were performed in Gaussian09 (unless noted)[26] at 298 K/1 atm. Ideal gas derived corrections from 1M standard state to 25 M water gave best agreement with experiment and are used throughout. See SI.

(24) (a) Zhao, Y.; Truhlar, D. G. *Acc. Chem. Res.* **2008**, *41*, 157-167; (b) Zhao, Y.; Truhlar, D. G. *Theor. Chem. Acc.* **2008**, *120*, 215-241.; (c) Tomasi, J.; Mennucci, B.; Cammi, R. *Chem. Rev.* **2005**, *105*, 2999-3094.

(25) Gonzalez, J.A., Ogba, O.M. Morehouse, G.F., Rosson, N., Houk, K.N., Leach. A.G., Cheong, P.H.Y., Burke, M. D., Lloyd-Jones, G. C. *Nat. Chem.* **2016**. DOI: 10.1038/NCHEM.2571.

(26) See SI for full authorship. (a) Gaussian 03, Revision **B.04**, Frisch, M. J., *et al.*, Gaussian, Inc., Wallingford CT, 2004; (b) Gaussian 09, Revision **C.01**, Frisch, M. J., *et al.* Gaussian, Inc., Wallingford CT, 2009.

(27) Lee, J. M.; Helquist, P.; Wiest, O. *J. Am. Chem. Soc.* **2012**, *134*, 14973-14981.

(28) Review: Renny, J. S.; Tomasevich, L. L.; Tallmadge, E. H.; Collum, D. B. *Angew. Chem. Int. Ed.* **2013**, *52*, 11998-12013.

(29) Kuivila reported added $B(OH)_3$ had no impact on rate,[17k] however as $[B]_{tot}$ ≤5 mM, k_2cat would be negligible.

(30) Marshall, W.; Franck, E. *J. Phys. Chem. Ref. Data* **1981**, *10*, 295-304.

(31) Cole, T. E.; Haly, B. D. *Organometallics* **1992**, *11*, 652-657.

(32) Formally the lower free energy boroxine-ate complexes provide the reference points for these reactions. However, for ease of comparison, the boronates are retained as zero point.

(33) As far as we aware, R_3B / $RB(OH)_2$ interconversion by a non-oxidative aqueous basic pathway has only been implicated as a side reaction in oxidation of 1,1-diboryl alkanes: Brown, H. C., Zweifel, G. *J. Am. Chem. Soc.* **1961**, *83*, 3834.

(34) (a) pK_{aH} **15-17**: Sadler, S. A.; Tajuddin, H.; Mkhalid, I. A. I.; Batsanov, A. S.; Albesa-Jove, D.; Cheung, M. S.; Maxwell, A. C.; Shukla, L.; Roberts, B.; Blakemore, D. C.; Lin, Z.; Marder, T. B.; Steel, P. G. *Org. Biomol. Chem.* **2014**, *12*, 7318-7327; (b) pK_{aH} **8**: Lezina, V. P.; Kozlova, M. M.; Gashev, S. B.; Stepanyants, A. U.; Smirnov, L. D. *Chem. Heterocycl. Compd.* **1986**, *22*, 903-914; (c) pK_{aH} **6**, **13**, **14**: Brisset, J.-L.; Ilimbi, V. *Can. J. Chem.* **1980**, *58*, 1250-1252.

(35) For processes that only impact at pH extremes (e.g. k'_3, k'_5) or where the heterocycle pK_{aH} <1, the values are overestimates.

(36) (a) Geissler, P. L., Dellago, C., Chandler, D., Hutter, J., Parrinello, M. *Science* **2001**, *291*, 2121–2124; (b) Gunaydin, H., Houk, K. N. *J. Am. Chem. Soc.* **2008**, *130*, 15232-15233.

(37) Beno, B. R.; Yeung, K.; Bartberger, M. D.; Pennington, L. D.; Meanwell, N. A. *J. Med. Chem.* **2015**, *58*, 4383-4438.

(38) For generation of 2-yridinium-carbenoids see: Ratts, K. W.; Howe, R. K.; Phillips, W. G. *J. Am. Chem. Soc.* **1969**, *91*, 6115-6121.

(39) For a related mechanistic proposal involving ylide liberation from the conjugate base of 2-pyridinium boronic acid (formal prototropy) see: Fuller, A. A.; Hester, H. R.; Salo, E. V; Stevens, E. P. *Tetrahedron Lett.* **2003**, *44*, 2935-2938.

(40) Ji, L.; Edkins, R. M.; Sewell, L. J.; Beeby, A.; Batsanov, A. S.; Fucke, K.; Drafz, M.; Howard, J. A. K.; Moutounet, O.; Ibersiene, F.; Boucekkine, A.; Furet, E.; Liu, Z.; Halet, J.-F.; Katan, C. Marder, T. B. *Chem. Eur. J.* **2014**, *20*, 13618-13635.

(41) (a) Li, Y.; Asadi, A.; Perrin, D. M. *J. Fluorine Chem.* **2009** *130*, 377-382; (b) Yan, J.; Springsteen, G.; Deeter, S.; Wang, B. *Tetrahedron*, **2004**, *60*, 11205-11209.

(42) a) Li, H., Zhong, Y.-L., Chen, C.-y., Ferraro, A. E., Wang, D. *Org. Lett.* **2015**, *17*, 3616; b) Chen, X., Ke, H., Chen, Y., Guan, C., Zou, G. *J. Org. Chem.* **2012**, *77*, 7572; c) Haag, B. A., Sämann, C., Jana, A., Knochel., P. *Angew. Chem. Int. Ed.* **2012**, *51*, 2667; d) Winkle, D. D., Schaab, K. M. *Org. Proc. Res. Dev.* **2001**, *5*, 450

(43) For ≥10% of maximum biomolecular reactivity (≥2.5% minor species), log [97.5/2.5] = 1.6; thus pH= pKa ±1.6

(44) (a) Molander, G. A.; Canturk, B.; Kennedy, L. A. *J. Org, Chem.* **2009**, *74*, 973-980; (b) Ren, W.; Li, J.; Zou, D.; Wu, Y.; Wu, Y. *Tetrahedron*, **2012**, *68*, 1351-1358.

Graphical Abstract